Vietnam Journal of Science and Technology ***60*** *(3) (2022) 468-477*

doi:10.15625/2525-2518/16385

EFFECT OF La ON THE STRUCTURE AND CHARACTERISTICS OF MULTIFERROIC $BiFeO_3$

Dao Son Lam[1, 2], Dinh Chi Linh[2], Ta Ngoc Bach[1], Dang Duc Dung[3], Ngo Thu Huong[4], Tran Dang Thanh[1, 2, *]

[1]*Graduate University of Science and Technology, Vietnam Academy of Science and Technology, 18 Hoang Quoc Viet, Cau Giay, Ha Noi, Viet Nam*

[2]*Institute of Materials Science, Vietnam Academy of Science and Technology, 18 Hoang Quoc Viet, Cau Giay, Ha Noi, Viet Nam*

[3]*School of Engineering Physics, Hanoi University of Science and Technology, 1 Dai Co Viet, Ha Ba Trung, HaNoi, Viet Nam*

[4]*Ha Noi University of Science, 334 Nguyen Trai, Thanh Xuan, Ha Noi, Viet Nam*

[*]Email: *thanhxraylab@yahoo.com*

Received: 15 August 2021; Accepted for publication: 4 February 2022

Abstract. $Bi_{1-x}La_xFeO_3$ (x = 0, 0.1, 0.2, 0.3) ceramics with a particle size of about 100 nm were prepared by high energy ball milling method and annealed at 800 ^oC in air for 6 h. Effects of La substitution on the structural, magnetic, ferroelectric, and optical properties of $BiFeO_3$ were examined in detail and systematically. The results indicate that partial replacement of Bi^{3+} by La^{3+} contributes to the formation of hexagonal single phase. Due to the increase of La^{3+} ion content, the values of the remnant polarization (P_r) and the coercive field (E_c) are improved, the maximum values achieved is about 0.0036 $\mu C/cm^2$ and 0.57 kV/cm, respectively, for sample x = 0.2. For increasing La doped content in $BiFeO_3$, the value of coercivity magnetic field (H_c) tends to decrease gradually. The optical property of $Bi_{1-x}La_xFeO_3$ ceramics was studied by analyzing their UV-vis absorption spectra. The value of band gap energy (E_g) of materials decreases from 1.86 to 1.78 eV, corresponding to x = 0 - 0.2, and the broad absorption band in the wavelength range of 660-700 nm. The observed characteristics of La-doped $BiFeO_3$ may be helpful for the further search for high-performance lead-free multiferroic magnetoelectric materials, oriented toward applications in solar cells, optoelectronic devices, or in the environmental pollution treatment technology field by the photocatalytic reaction.

Keywords: Multiferroic, magnetic property, ferroelectric property, optical property.

Classification numbers: 2.2.2, 2.5.1, 2.9.2.

1. INTRODUCTION

Multiferroic materials refer to a class of materials which possess the intrinsic coupling of two or more ferroic orders (ferroelectric, ferroelastic, and ferromagnetic). Among them, magnetoelectric materials exhibiting both ferroelectric and ferromagnetic characteristics have

received much attention due to their great potential in multifunctional applications such as spintronics, memory, and sensors [1 - 5]. The magnetoelectric coupling between two order parameters makes it possible to manipulate the polarization states by external magnetic fields or opposite. Recent publications on multiferroic materials with single phase structure have shown that $BiFeO_3$ (BFO) is an ideal candidate which shows unambiguous room temperature magnetoelectric coupling effect with a Curie temperature of 1103 K and a Néel temperature of 643 K [4 - 7]. The conductivity of the material changes abnormally at the Neél temperature T_N, the magnetic electrical properties are closely related, showing that the BFO material has the magnetic-electric effects [8 - 10]. Suitable ionic doping onto Bi or Fe-sites in the BFO structure has been widely accepted to improve their magnetic, electric, and magnetoelectric properties. Because of these features and good optical properties, pure and doped BFO are considered highly promising candidates for practical applications in next-generation smart materials. BFO material is a photocatalyst enhanced through doping to reduce its band-gap (2.8-1.3 eV) [9 - 13]. This material has proven to be very useful for the degradation of dyes under visible light irradiation among other photocatalysts. Its exceptional nontoxicity, suitability, low cost and long term excellent stability make it an efficient photocatalyst for the degradation of effluents from textile and pharmaceutical industries which ended-up in the environment and is now a major concern of the modern world [8]. Research on advanced materials in environmental remediation and pollutant degradation is progressing rapidly because of their wide variety of applications. The photocatalytic activity of BFO nanoparticles is a promising field of research in photocatalysis. The doping effects of BFO and other related materials have shown greatly improved photoactivity under visible light response [14, 15]. Recent studies have shown that, when BFO ceramics are annealed at high temperature the oxygen vacancies in their structure will appear. The saturation magnetization value is proportional to the number of oxygen vacancies in the BFO ceramics, exhibiting a weak ferromagnetic order [9]. In addition, the electromagnetic properties of BFO have been improved by substituting rare earth ions (La^{3+} [16], Pr^{3+} [17], Sm^{3+} [9], Sr^{3+} [18]) at Bi-site and transition metal (Mn [4], Co [6], Ti [17] at Fe-site [3-9]. The introduction of rare-earth ions, particularly for the case of La-doped BFO, has been demonstrated to exhibit favorable results [16, 19]. The increase in spin canting angle and the magnetic phase transition may be the main origin of weak ferromagnetism in La doped BFO. Especially when doped with only La, the material exhibits a weak ferromagnetic character. The maximum value of magnetization was reported as only 0.2 emu/g under an applied magnetic field of 50 kOe [16]. The optical band gap was found to decrease with La doping [16]. In 2020, Anju Kumari *et al*. studied and successfully fabricated La doped BFO with a doping concentration of $x = 0$ - 0.05 [19]. They showed that the average particle size was estimated to be in the range of 30 - 50 nm. As the doping concentration increases from $x = 0$ to $x = 0.05$, the residual polarization and coercive electric field significantly increased from 0.15 to 1.0 $\mu C/cm^2$ and from 10.19 to 42.87 kV/cm, respectively [19]. The value of the band gap energy decreases with increasing impurity concentration. For $x = 0.05$, the value of E_g reaches approximately 1.83 eV [19]. Nowadays, BFO can be prepared by many different methods such as sol-gel [9, 20], co-precipitation [21], combustion [22], and high energy ball milling [23]. Especially, when multiferroic materials are fabricated by high energy ball milling method, due to the influence of lattice distortion, the surface defects are usually large, and the residual electrical polarization is thus often significantly improved [14, 18, 23]. However, studies on the effect of La substitution on structural, electric, magnetic and optical properties of BFO nanoparticles (NPs) prepared by using high energy ball milling method have not been done in detail and systematically. This triggered us to synthesize $Bi_{1-x}La_xFeO_3$ ($x = 0$, 0.1, 0.2, 0.3) NPs and investigate their structural, magnetic, ferroelectric and optical properties.

2. MATERIALS AND METHODS

$Bi_{1-x}La_xFeO_3$ (BLF) ceramics with x = 0, 0.1, 0.2, 0.3 (denoted as BFO, BLF1, BLF2, BLF3, respectively) were prepared from high purity (99.9 %) powders of Bi_2O_3, Fe_2O_3 and La_2O_3 by a combination of high energy ball milling and thermal processing methods. Firstly, the mass of precursors was calculated and weighed according to nominal formulas to create BLF compounds via the high energy ball milling method on a Spex-8000D machine for 5 h in air. After that, the powdered mixture of each compound were pressed into pellets with a diameter of 12 mm and a thickness of 1.5 mm under a pressure of 7000 kg/cm^2, and then annealed for 6 h at 800 °C in air.

The crystal structure and the particle size of the composites were checked by X-ray diffraction (XRD) patterns using an Equinox 5000 device (Thermo Scientific, Cu-K_α radiation with λ = 1.54056 Å) and scanning electron microscopy (SEM) images via a Fe-SEM S4800 instrument (Hitachi), respectively. The ferroelectric and magnetic properties were investigated through the hysteresis curves measured on a Model 609 Precision LC II and a vibrating sample magnetometer, respectively. UV-vis absorption spectra were measured on a UV-vis-NIR Cary 5000 instrument. All of the measurements were performed at room temperature.

3. RESULTS AND DISCUSSION

Figure 1 shows the XRD patterns of $Bi_{1-x}La_xFeO_3$ (x = 0, 0.1, 0.2, 0.3) ceramics. The X-ray diffraction patterns of BLF ceramics show some low peaks corresponding to the secondary phase of $Bi_2Fe_4O_9$ for the BFO sample (x = 0), which are denoted by an asterisk (*) [7]. However, La-doped BFO samples exhibit a single phase of BLF, corresponding to a perovskite structure. These patterns are suitable for a JCPDS card No. 01-075-6667. All XRD peaks of BLF phase are designated by the Miller indices (*hkl*) ((012), (104), (110), (006), (202), (024), (116), (122), (018), (214)), which belong to a hexagonal structure (space group: *R*3*c*). This is consistent with previous studies [16, 19]. Our results suggest that La doped into the BFO host lattice contributes to the fabrication a single phase of BLF.

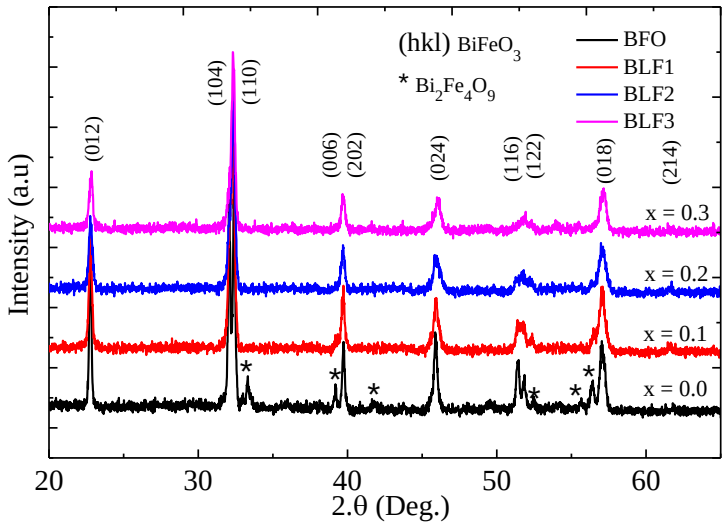

Figure 1. X-ray diffraction patterns of BLF ceramics.

To obtain information about the morphology, particle size, and the percentage of elements of our samples, SEM images and X-ray energy dispersion spectroscopy (EDX) were performed.

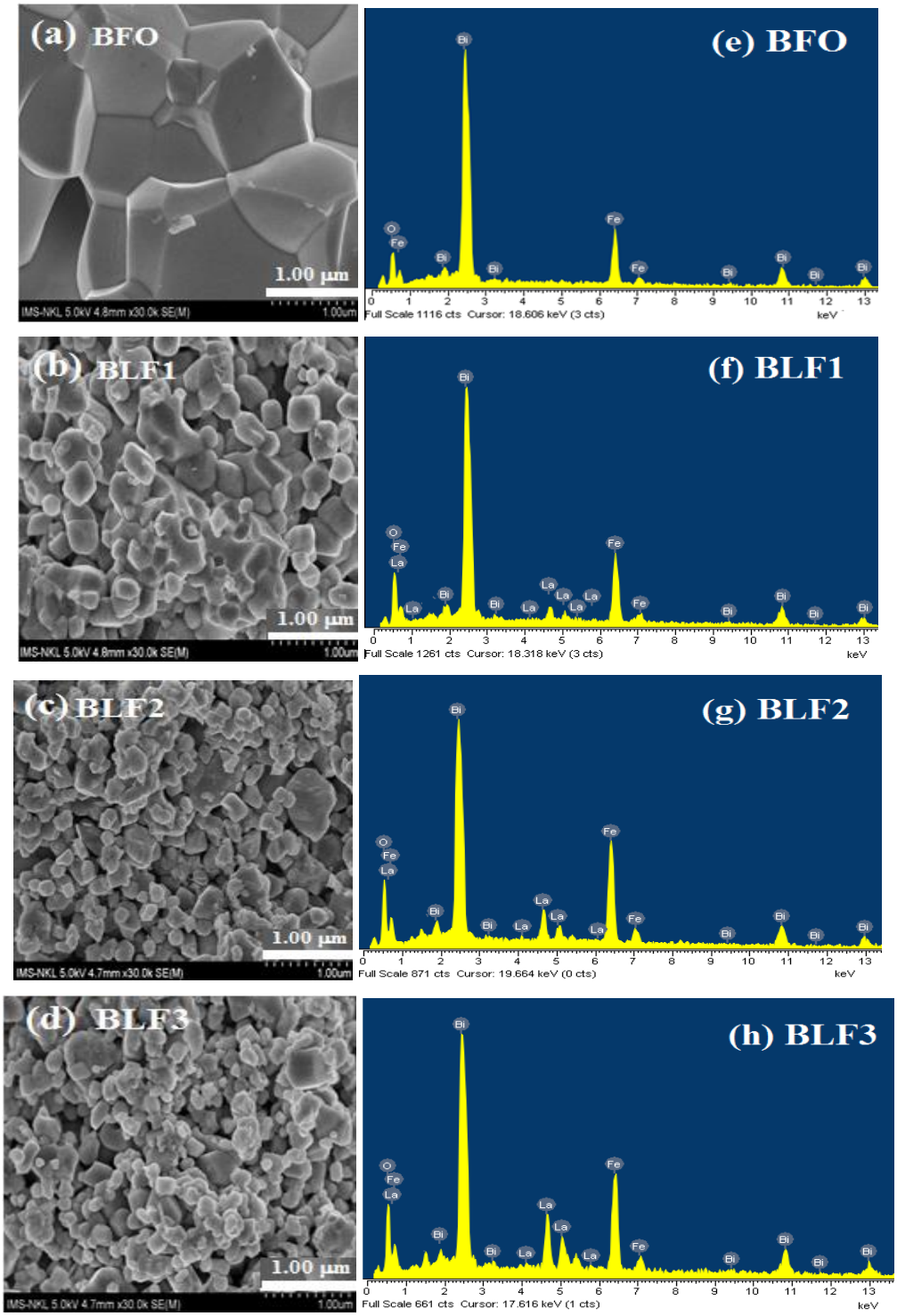

Figure 2. SEM images (a-d) and EDX spectra (e-h) for BLF ceramics.

Figure 2 presents SEM images and EDX spectra for BLF samples with different La contents. As shown in Figures 2(a-d) for the SEM images, the x = 0 sample exhibits a rather large particle size of about 1 μm. Meanwhile, the La-doped samples show the particles of polyhedral shape with smaller size, which is found to be about 100 - 200 nm and tends to decrease with increasing La concentration. Based on EDX spectra shown in Figures 2(e-h), we find a full presence of the elements Bi, Fe, O and La in the samples. All of them are in the precursors. It means that there should be no contamination of all the samples during fabrication. In addition, the intensity of the EDX lines corresponding to La element gradually increased in accordance with an addition of La concentration in the samples. Figure 3 shows the magnetic field dependence of magnetization for BLF ceramics measured at room temperature. Figures 3(a-d) show that the hysteresis curves $M(H)$ and the shape $M(H)$ curves exhibit a coexistence of the diamagnetic and weak ferromagnetic characters. The value of saturation magnetization of the samples is quite small. In the high magnetic field range (above 3000 Oe), the $M(H)$ curves show a diamagnetic signal.

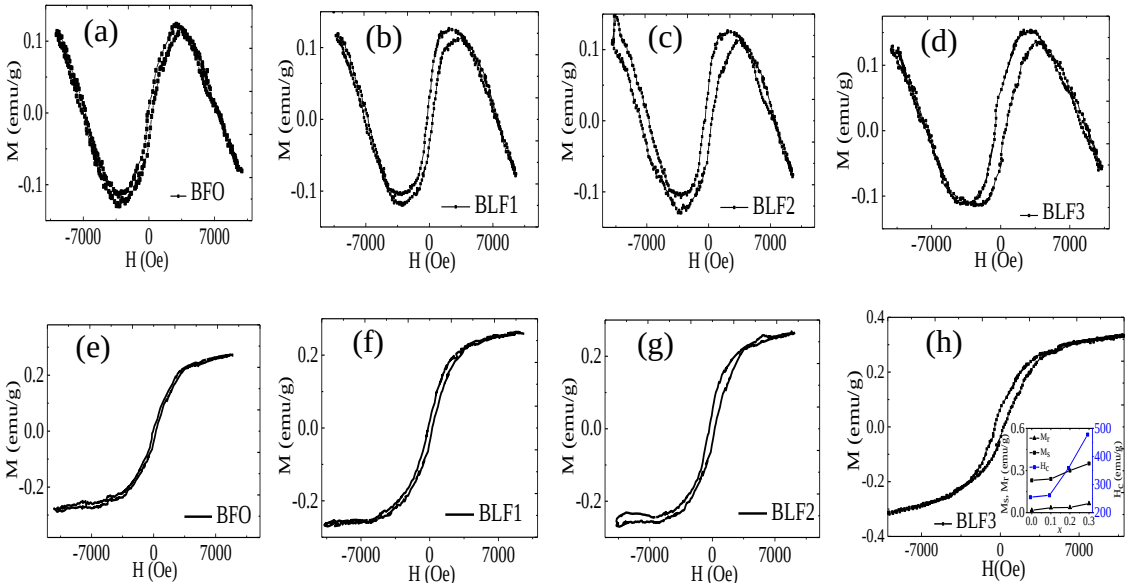

Figure 3. Magnetic hysteresis curves for BLF ceramics before (a-d) and after (e-h) removing the diamagnetic part. The insert in Figure 3(h) shows M_s, M_r, and H_c versus x.

In order to estimate the contribution of the weak ferromagnetic phase, the diamagnetic signal in $M(H)$ curves has been extracted. To subtract the diamagnetic signal, the linear $M(H)$ data at high field were used to fit to a linear function, which is considered as the contribution of the diamagnetic part in the samples. The contribution of the weak ferromagnetic part can be obtained after extracting the diamagnetic part. As presented in Figures 3(e-h), $M(H)$ curves of samples after correction exhibit the hysteresis characters of the weak ferromagnetic part with quite small magnetization. According to recent reports, the origin of the weak ferromagnetic contribution in BFO compounds could be related to the antiferromagnetic interaction of Fe^{3+} ions [4, 7, 9]. Partial substitution of Bi^{3+} by rare-earth ions will contribute to the enhancement of magnetization in the material. Similar to the BFO ceramics doped with other rare earths (Nd, Dy) [3, 7, 12], the remnant magnetization (M_r) gradually increases with increasing La^{3+} concentration. The variation of the saturation magnetization (M_s), the remnant magnetization

(M_r), and the coercive field ($H_{c)}$ is plotted as a function of La content (x) in the BLF ceramics and is shown in the inset of Figure 3(h). As the La doped concentration gradually increases, the values of M_s, M_r, and H_c are significantly improved. Namely, the values of M_s, M_r, and H_c are found to be 0.23-0.35 emu/g, 0.017-0.065 emu/g, and 255-478 Oe for x = 0-0.3, respectively. The spiral spin structure of BFO is suppressed by the substitution of La^{3+} ions for Bi^{3+} ions which leads to structural distortion giving rise to an enhanced magnetization [3, 7, 16, 19]. Figures 4(a-c) show the ferroelectric hysteresis loops for pure BFO and La doping of BFO ceramics measured under the maximum voltages (V_{max}) of 100, 500, and 1000 V at room temperature. All BLF ceramics exhibit a ferroelectric character.

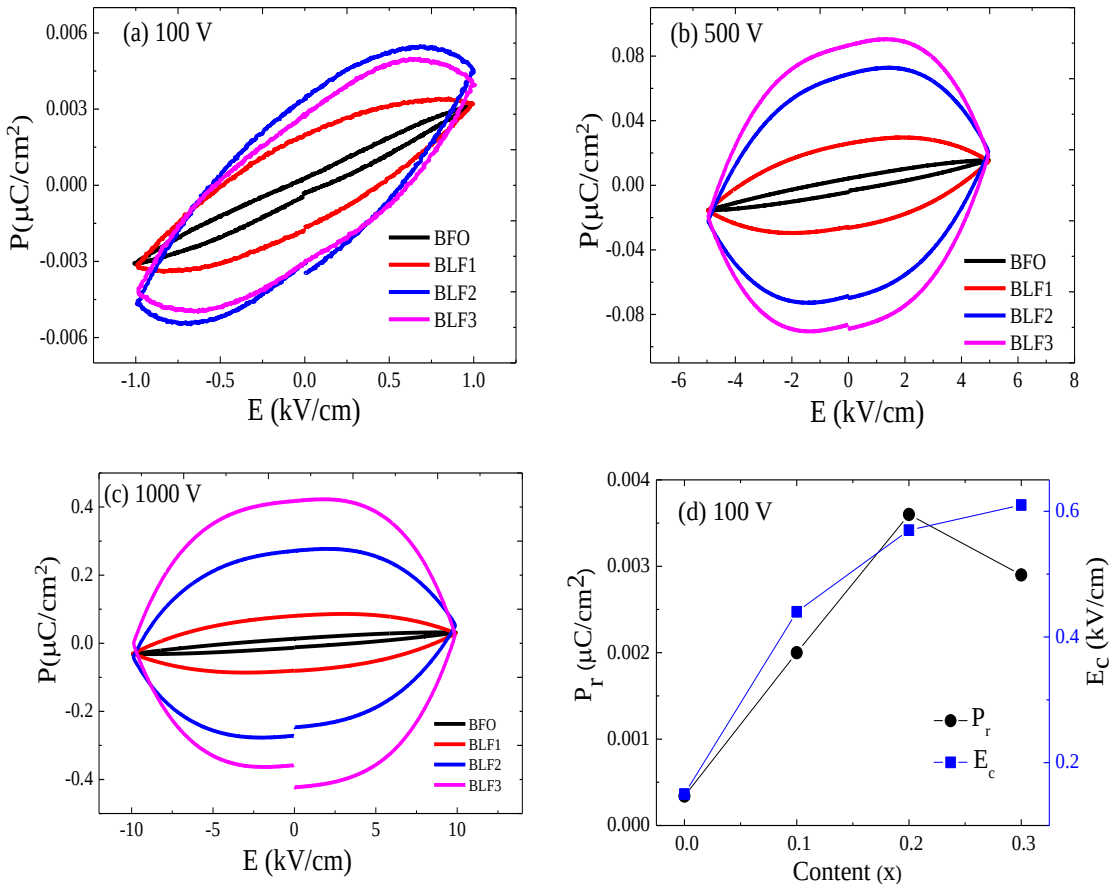

Figure 4. Hysteresis $P(E)$ curves of the BLF ceramics under the maximum voltages of 100 (a), 500 (b), and 1000 V (c), and P_r, E_c values determined under the maximum voltage of 100 V (d).

At the electric field generated by a voltage of 100 V, the $P(E)$ curves have the typical form of a ferroelectric material, and have not been degraded. It is striking that only a La^{3+} substitution can dramatically change the electric polarization behavior. As the La doped concentration gradually increases, the values of residual electrical polarization (P_r) and coercive electric field (E_c) are significantly improved. Specifically, the value of P_r reaches its maximum of about 0.0036 $\mu C/cm^2$ corresponding to x = 0.2 and then decreases for x = 0.3. The coercivity increased with the La content (x), the values of E_c was found to be 0.15-0.61 kV/cm for x = 0-0.3, respectively. This is shown in detail in Figure 4(d). At a higher applied voltage (about 500 V),

the $P(E)$ curves of samples are not similar to the theoretical curves of ferroelectric materials. They exhibit the degenerate patterns, commonly referred to as the fingerprint pattern. For the degeneracy curves, it is impossible to determine the saturation polarization. This degradation can be explained by the relative leakage current in the samples. Therefore, only low field electric hysteresis loops have been obtained. The relatively high conductivity of $BiFeO_3$ is known to be attributed to the variable oxidation states of Fe ions (from Fe^{3+} to Fe^{2+}), which require oxygen vacancies for charge compensation [9, 19]. The presence of Fe^{2+} ions and oxygen deficiency lead to high conductivity [11]. As mentioned above, The doping of La onto BFO not only affects its structural characteristics, but also significantly improves its electrical and magnetic properties. The effect of improving the multiferroic properties of the material is evident through the increase in the residual electrical polarization and residual magnetism of the material [14]. Besides, the influence on electrical and magnetic properties of the material can also cause a change in the typical optical property of this system. The optical property of samples were studied by analyzing their UV-vis absorption spectra. The absorption spectra of the BLF ceramics transformed from diffuse reflection spectra based on Kubelka-Munk theory are presented in Figure 5

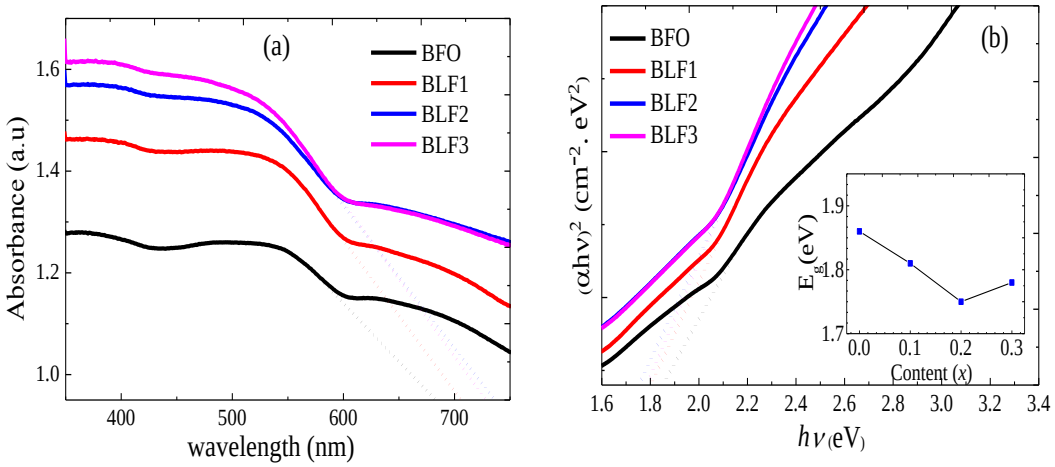

Figure 5. Ultraviolet and visible light absorbance of BLF ceramics (a) and the relationship between $(\alpha hv)^2$ and hv (b). The inset in Fig. 5(b) shows the dependence of E_g on the La-doped concentration.

As shown in Figure 5, the absorption spectra of the BLF ceramics with different La doping show that BLF ceramics can absorb considerable amounts of visible light, suggesting their utilization for potential applications. Moreover, compared with the pure BFO sample, La-doped BFO samples show higher visible light absorption. The broad absorption band in the wavelength range of 660-700 nm is attributed to the crystal field transition [7, 8]. The band gap energy (E_g) can be determined using the equation: $(\alpha hv)^n = A(hv - E_g)$ where, α is the absorption coefficient, λ is the wavelength, A is a constant, and the exponent n is a constant. Based on the experimental data, we find $n = 2$ that is suitable for the BTO system [23 - 28], which is quite suitable for our samples. From Figure 5(b), construct the tangent lines of the most linear segment on the lines $(\alpha hv)^2$ according to hv and extrapolate the value $(\alpha hv)^2 = 0$, we will determine the E_g value of the respective samples. The E_g values are estimated to be 1.86, 1.81, 1.75, and 1.78 eV for the samples with $x = 0$, 0.1, 0.2, and 0.3, respectively. These values are consistent with the reported values for pure and doped BFO [7, 10, 19, 28 - 30]. Therefore, they are smaller than those reported for BFO thin film and BFO nanoparticles [4, 26, 27, 31]. The band gap energy of BLF

ceramics appropriating in visible region indicates the possibility of their utilization for photocatalysis and other optical device applications. The decrease in band gap energy of BLF samples may be attributed to the rearrangement of molecular orbitals and distortion induced in the FeO_6 octahedra [31], . making BLF composites become more helpful for the photocatalytic and solar cell applications.

4. CONCLUSIONS

$Bi_{1-x}La_xFeO_3$ ceramics (x = 0, 0.1, 0.2, 0.3) with a hexagonal structure were successfully prepared by using a combination of high-energy ball milling and thermal processing methods. It can be concluded that La doping is an effective way to improve the single phase of ceramics, as well as the multiferroic and optical characters. With increasing the content of La^{3+} ions, the values of the saturation magnetization (M_s) and the residual magnetization (M_r) gradually increased, meanwhile, the remnant polarization (P_r) reached the maximum value corresponding to the La-doped concentration of x = 0.2. Additionally, the value of band gap energy (E_g) obtained for the samples also decreased and reached a minimum value of 1.75 eV for x = 0.2. With optical band gap in visible region, La doped $BiFeO_3$ ceramics are a potential material for optoelectronic device and solar cell applications.

Acknowledgements. This research is funded by Graduate University of Science and Technology under grant number GUST.STS.ĐT2020-KHVL02.

CRediT authorship contribution statement. Dao Son Lam: Project administration, Formal analysis, Investigation, Writing - review & editing. Dinh Chi Linh: Investigation, Formal analysis. Ta Ngoc Bach: Investigation, Dang Duc Dung: Investigation. Ngo Thu Huong: Investigation. Tran Danh Thanh: Conceptualization, Investigation, Review & editing, Supervision.

Declaration of competing interest. The authors declare that they have no known competing financial interests or personal relationships that could have appeared to influence the work reported in this paper.

REFERENCES

1. Wang N., Luo X., Han L., Zhang Z., Zhang R., Olin H. & Yang Y. - Structure, performance, and application of $BiFeO_3$, Nano-Micro Lett. **12** (2020) 81. https://doi.org/10.1007/s40820-020-00420-6.
2. Ihlefeld J. F., Podraza N. J., Liu Z. K., Rai R. C., Xu X., Heeg T., Chen Y. B., Li J., Collins R. W., Musfeldt J. L., Pan X. Q., Schubert J., Ramesh R., and Schlom D. G. - Optical band gap of $BiFeO_3$ grown by molecular - beam epitaxy, Appl. Phys. Lett. **92** (14) (2008) 142908. https://doi.org/10.1063/1.2901160.
3. Oliveira R. C., Volnistem E. A., Astrath E. A. C., Dias G. S., Santos I. A., Garcia D., Eiras J. A. - La Doped $BiFeO_3$ ceramics synthesized under extreme conditions: Enhanced magnetic and dielectric properties, Ceram. Int. **47** (14) (2021) 20407-20412. https://doi.org/10.1016/j.ceramint.2021.04.049.
4. Liu Y., Tan G., Ren X., Li J., Xue M., Ren H. Xia A., Liu W. - Electric field dependence of ferroelectric stability in $BiFeO_3$ thin films co-doped with Er and Mn, Ceram. Int. **46** (11) (2020) 18690-18697. https://doi.org/10.1016/j.ceramint.2020.04.183.
5. Chakrabarti K., Das K., Sarkar B., Ghosh S., De S. K., Sinha G., Lahtinen J. - Enhanced magnetic and dielectric properties of Eu and Co co-doped $BiFeO_3$ nanoparticles, Appl. Phys. Lett. **101** (4) (2012) 042401. https://doi.org/10.1063/1.4738992.

6. Liu J., Li M., Pei L., Wang J., Hu Z., Wang X., Zhao X. - Enhanced magnetic and dielectric properties of Eu and Co co-doped $BiFeO_3$ nanoparticles, Appl. Phys. Lett. **101** (4) (2012) 042401. https://doi.org/10.1063/1.4738992.
7. Sati P. C., Arora M., Chauhan S., Kumar M., Chhoker S. - Effect of Dy substitution on structural, magnetic and optical properties of $BiFeO_3$ ceramics, J. Phys. Chem. Solids. **75** (1) (2014) 105-108. http://dx.doi.org/10.1016/j.jpcs.2013.09.003.
8. Sakar M., Balakumar S., Saravanan P., Bharathkumar S. - Compliments of confinements: substitution and dimension induced magnetic origin and band bending mediated photocatalytic enhancements in $Bi_{1-x}Dy_xFeO_3$ particulate and fiber nanostructures, Nanoscale **7** (24) (2015) 10667-10679. https://doi.org/10.1039/C5NR01079A.
9. Gu Y., Zhou Y., Zhang W., Guo C., Zhang X., Zhao J., Zhang Y., and Zheng H. - Optical and magnetic properties of Sm-doped $BiFeO_3$ nanoparticles around the morphotropic phase boundary region, AIP Advances **11** (4) (2021) 045223. https://doi.org/10.1063/5.0042485.
10. Gao F., Chen X. Y., Yin K. B., Dong S., Ren Z. F., Yuan F., Yu T., Zou J., Liu M. - Visible-Light photocatalytic properties of weak magnetic $BiFeO_3$ nanoparticles, Adv. Mater. **19** (19) (2007) 2889-2892. https://doi.org/10.1002/adma.200602377.
11. Irfan S., Zhuanghao Z., Li F., Chen Y. X., Liang G. X., Luo J. T., Ping F. - Critical review: Bismuth ferrite as an emerging visible light active nanostructured photocatalyst, J. Mater. Res. Technol. **8** (6) (2019) 6375-6389. https://doi.org/10.1016/j.jmrt.2019.10.004.
12. Chen Z., Wu Y., Wang X., Jin W., Zhu C. - Ferromagnetism and enhanced photocatalytic activity in Nd doped $BiFeO_3$ nanopowders, J. Mater. Sci. Mater. Electron. **26** (12) (2015) 9929–9940. https://doi.org/10.1007/s10854-015-3669-9.
13. Mocherla P. S. V., Karthik C., Ubic R., Ramachandra Rao M. S., and Sudakar C. - Tunable bandgap in $BiFeO_3$ nanoparticles: The role of microstrain and oxygen defects, Appl. Phys. Lett **103** (2) (2013) 022910. https://doi.org/10.1063/1.4813539.
14. Jiang Q., Ning H., Zhang Q., Cain M., Reece M. J., Yan H. - Active ferroelectricity in nanostructured multiferroic $BiFeO_3$ bulk ceramics, J. Mater. Chem. C. **1** (36) (2013) 5628-5631. https://doi.org/10.1039/C3TC31140F.
15. Haruna A., Abdulkadir I., Idris S. O. - Effect of annealing temperature on the synthesis and photocatalytic properties of $Bi_{0.65}K_{0.2}Ba_{0.15}FeO_3$ perovskite-like nanoparticle synthesized by sol-gel method, Beni-Suef Univ. J. Basic Appl. Sci. **6** (2020) 03237. https://doi.org/10.1186/s43088-020-0033-9.
16. Lazenka V. V., Ravinski A. F., Makoed, Vanacken J., Zhang G., Moshchalkov V. V. - Weak ferromagnetism in La-doped $BiFeO_3$ multiferroic thin films, J. Appl Phys. **111** (12) (2012) 123916. https://doi.org/10.1063/1.4730896.
17. Sati P.C., Arora M., Chauhan S., Kumar M., Chhoker S. - Structural, magnetic, vibrational and impedance properties of Pr and Ti codoped $BiFeO_3$ multiferroic ceramics, Ceram. Int. **40** (6) (2014) 7805-7816. http://dx.doi.org/10.1016/j.ceramint.2013.12.124.
18. Daneshmand N., Shokrollahi H., Lavasani S.A.N.H. - Enhanced magnetic and dielectric properties in bismuth ferrite ($Bi_{2-x}Sr_xFe_4O_9$) derived by the reverse chemical co-precipitation method, J. Mater. Sci.: Mater. Electron. **29** (2018) 3201–3209. https://doi.org/10.1007/s10854-017-8255-x.
19. Kumari A., Kumari K., Ankush V., Alvi P. A., and Kumar S. - Electrical and Structural Properties of La doped $BiFeO_3$, AIP Conf. Proc. **2220** (1) (2020) 040032. https://doi.org/10.1063/5.0001563.

20. Gaur A., Singh P., Choudhary N., Kumar D., Shariq M., Singh K., Kaur N., and Kaur D. - Structural, optical and magnetic properties of Nd-doped $BiFeO_3$ thin films prepared by pulsed laser deposition, J. Phys. B. **406** (10) (2011) 1877-1882. http://dx.doi.org/10.1016/j.physb.2011.02.046.
21. Mardani R. - The synthesis of Ba^{2+}-doped multiferroic $BiFeO_3$ nanoparticles using co-precipitation method in the presence of various surfactants and the investigation of structural and magnetic features, Mod. Phys. Lett. B **31** (15) (2017) 1750169. https://doi.org/10.1142/S021798491750169X.
22. Lam S. M, Sin J., Mohamed. A.R. - A newly emerging visible light-responsive $BiFeO_3$ perovskite for photocatalytic applications: a mini review, Mater. Res. Bull. **90** (2017) 15–30. https://doi.org/10.1016/j.materresbull.2016.12.052.
23. Pedro-García F., Sanchez-De Jesús F., Cortes-Escobedo C. A., Barba-Pingarron A. M., Bolarín-Miro A. - Mechanically assisted synthesis of multiferroic $BiFeO_3$: Effect of synthesis parameters, J. Alloys Compd. **711** (2017) 77-84. http://dx.doi.org/10.1016/j.jallcom.2017.03.292.
24. Jaffari Z. H., Lam S. M., Sin J. C., Zeng H., Rahman M. A. - Magnetically recoverable Pd-loaded $BiFeO_3$ microcomposite with enhanced visible light photocatalytic performance for pollutant, bacterial and fungal elimination, Separ. Purif. Technol. **236** (2020) 116195. https://doi.org/10.1016/j.seppur.2019.116195.
25. Muneeswaran M. and Giridharan N. V. - Effect of Dy-substitution on the structural, vibrational, and multiferroic properties of $BiFeO_3$ nanoparticles, J. Appl. Phys. **115** (21), (2014) 214109. https://doi.org/10.1063/1.4881529.
26. Sando D., Carrétéro C., Grisolia M. N., Barthélémy A., Nagarajan V., and Bibes M. - Revisiting the optical band gap in epitaxial $BiFeO_3$ thin films, Adv. Optical Mater. **6** (2) **(**2017) 1700836. https://doi.org/10.1002/adom.201700836.
27. Bhushan B., Basumallick A., Bandopadhyay S. K., Vasanthacharya N. Y., Das D. - Effect of alkaline earth metal doping on thermal, optical, magnetic and dielectric properties of $BiFeO_3$ nanoparticles, J. Phys. D: Appl. Phys. **42** (6) (2009) 065004. https://doi.org/10.1088/0022-3727/42/6/065004.
28. Mukherjee A., Hossain S. M., Pal M., Basu S. - Effect of doping on optical properties of multiferroics $BiFeO_3$ nanoparticles, Appl. Nanosci. **2** (2012) 305. https://doi.org/10.1007/s13204-012-0114-8.
29. Haruna A., Abdulkadir I., Idris S. O., Heliyon. - Photocatalytic activity and doping effects of $BiFeO_3$ nanoparticles in model organic dyes, Heliyon. **6** (2020) 03237. https://doi.org/10.1016/j.heliyon.2020.e03237.
30. Bhushan B., Basumallick A., Vasanthacharya N. Y., Kumar S., Das D. - Sr induced modification of structural, optical and magnetic properties in $Bi_{1-x}Sr_xFeO_3$ (x = 0, 0.01, 0.03, 0.05 and 0.07) multiferroic nanoparticles, Solid State Sci. **12** (7) (2010) 1063-1069. https://doi.org/10.1016/j.solidstatesciences.2010.04.026.
31. Chen P., Xu X., Koenigsmann C., Santulli A. C., Wong S. S., Musfeld J. L. - Size-Dependent infrared phonon modes and ferroelectric phase transition in $BiFeO_3$ nanoparticles, Nano Lett. **10** (11) (2010) 4526-4532. https://doi.org/10.1021/nl102470f.